ACADEMIC PRESS

Available online at www.sciencedirect.com

SCIENCE DIRECT®

Journal of Sound and Vibration 265 (2003) 337–358

JOURNAL OF SOUND AND VIBRATION

www.elsevier.com/locate/jsvi

Extension of SEA model to subsystems with non-uniform modal energy distribution

L. Maxit*, J.-L. Guyader

Vibrations - Acoustic Laboratory, INSA de Lyon, National Institute of Applied Sciences, 25 bis, Avenue Jean Capelle, 69621 Villeurbanne, Cedex, France

Received 30 July 2001; accepted 3 July 2002

Abstract

In order to widen the application of statistical energy analysis (SEA), a reformulation is proposed. Contrary to classical SEA, the model described here, statistical modal energy distribution analysis (SmEdA), does not assume equipartition of modal energies.

Theoretical derivations are based on dual modal formulation described in Maxit and Guyader (Journal of Sound and Vibration 239 (2001) 907) and Maxit (Ph.D. Thesis, Institut National des Sciences Appliquées de Lyon, France 2000) for the general case of coupled continuous elastic systems. Basic SEA relations describing the power flow exchanged between two oscillators are used to obtain modal energy equations. They permit modal energies of coupled subsystems to be determined from the knowledge of modes of uncoupled subsystems. The link between SEA and SmEdA is established and make it possible to mix the two approaches: SmEdA for subsystems where equipartition is not verified and SEA for other subsystems.

Three typical configurations of structural couplings are described for which SmEdA improves energy prediction compared to SEA: (a) coupling of subsystems with low modal overlap, (b) coupling of heterogeneous subsystems, and (c) case of localized excitations.

The application of the proposed method is not limited to theoretical structures, but could easily be applied to complex structures by using a finite element method (FEM). In this case, FEM are used to calculate the modes of each uncoupled subsystems; these data are then used in a second step to determine the modal coupling factors necessary for SmEdA to model the coupling.

*Corresponding author. Tel.: +33-4-72-438080; fax: +33-4-72-438712.
E-mail address: maxit@lva.insa-lyon.fr (L. Maxit).

0022-460X/03/$ - see front matter
doi:10.1016/S0022-460X(02)01459-1

1. Introduction

Statistical energy analysis (SEA) [1–5] has been developed to predict noise and vibration transmission through complex structures at medium and high frequencies. In SEA, the structure is subdivided into a number of subsystems and the vibration response within each subsystem is characterized by the subsystem energy. Derivation of SEA is based on several assumptions (see Ref. [6]), and its range of validity is not easy to establish although many studies have addressed this issue [7–29]. A number of cases where SEA is not a good predictor will be discussed.

Yap and Woodhouse [7] studied the influence of damping on the quality of SEA results. Equivalent coupling loss factor (CLF) was obtained from numerical simulations on beam and plate coupling, which were shown to depend strongly on damping, whereas CLF obtained classically by the wave approach were independent of damping. For weakly damped system, equivalent CLFs are proportional to damping loss factors (DLF), and values are lower than those given by the wave approach; i.e., the wave approach appears to overestimate the energy transfer. The authors attributed the strong dependency to damping to the fact that energy equipartition does not hold when damping is low.

For three plates coupled in a U shape, Fredo [8] showed that indirect coupling between the first and third plate can be significant if damping is weak. The indirect coupling was attributed to the inaccuracy of one or more SEA assumptions. Previously, Finnveden had shown in the case of three coupled elements [9] that SEA seriously overestimates the flow of energy when damping loss factors are small.

The coupling of two irregular plates has been studied by Mace et al. [10,11]. For strong damping, the response is independent of the shape of the plate and the wave estimate of CLF gives accurate predictions. Contrary to weak damping, the transmission depends significantly on the specific geometry of each plate and the power transmitted is often substantially less than that predicted by SEA.

Ming and Pan studied the accuracy of SEA results on coupled plates [12]. They observed that two parameters influence the quality result: the geometric mean of the modal overlap factors and the number of resonant modes in the frequency band of interest. At low frequency, where there are few modes, SEA results are poor and exact results are highly sensitivite to the position of the excitation point. Increasing frequency, modal overlap factors and mode numbers increase when SEA results are better and sensitivity to the position of excitation decreases (see also Ref. [13]). Previous work by Fahy and Mohammed [14] on beam–plate coupling gave similar conclusions. When the modal overlap factor is much less than unity, SEA overestimates energy transfer. From analytical calculations of the power exchanged by two coupled one-dimensional subsystems, Mace [15,16] suggested that the γ parameter could characterize the coupling strength. This parameter is defined as the ratio of the transmission factor to the product of the two modal overlap in both connected subsystem. When γ is small, the coupling is called weak, i.e., classical SEA is valid. Finnveden [17,18] deduced the same coupling strength criterion by investigating the ensemble averaged power flow in a three elements structure.

It can be concluded that it is difficult to predict energy transfer when SEA assumptions are not verified in at least one subsystem. The key point of the present study was refining SEA, based on less restrictive assumptions.

Langley [19,20] proposed an extension of SEA called wave intensity analysis (WIA). Classical SEA assumed that the vibrational wavefield in each subsystem is diffuse. In some cases (not explicitly defined by the author), this assumption cannot be fulfilled which means that SEA yields poor estimates of vibrational responses. In WIA, the directional dependency of the vibrational wavefield in each subsystem is derived using Fourier series. When only the first term of the Fourier series is considered, WIA is equivalent to SEA. Adding terms in the series improves predictions for plate assemblies [19–22].

The study presented in this paper is also based on the reformulation of SEA with less restrictive assumptions. The goal is to extend the validity of the model to cases where classical SEA was seen to be unsatisfactory. The assumption that one wishes to remove in this paper is equipartition of energy. The approach, based on the dual modal formulation proposed in Refs. [1,2], takes into account the modal energies distribution of each subsystem. The present model is called statistical modal energy distribution analysis (SmEdA) and can be seen as a refinement of traditional SEA.

2. Dual modal formulation

The dual modal formulation described in Ref. [1] for the general case of coupled continuous elastic systems is based on a dual displacement–stress formulation and two kinds of subsystem modes: uncoupled-free modes and uncoupled-blocked modes. The results which constitute the base of SmEdA model are summarized here. (For more details, see Refs. [1,2].)

2.1. Coupling of two continuous mechanical systems

Two elastic continuous mechanical sub systems are considered which are rigidly coupled on a surface $S_{Coupling}$ as shown in Fig. 1. Both systems are excited by random, ergodic excitations of

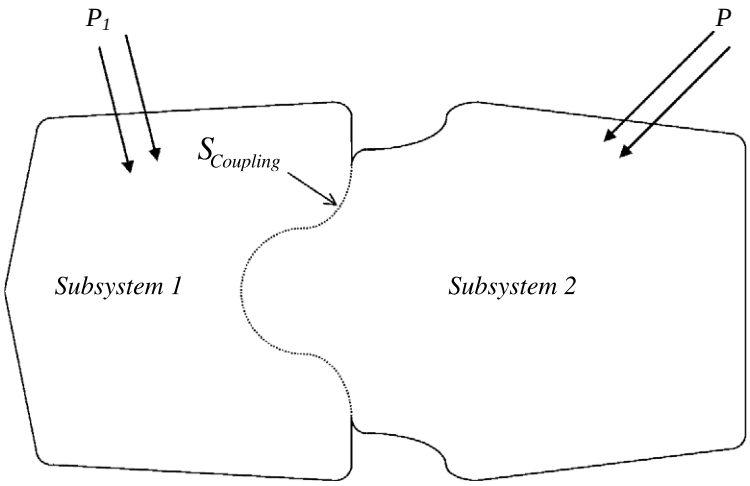

Fig. 1. Coupling of two continuum mechanical systems.

band-limited white-noise type and the material of each subsystem is supposed to be linear elastic and to have viscous damping.

Subsystem 1 is described by displacement vector $W_i(M, t)$ and subsystem 2 by stress tensor $\sigma_{ij}(M', t)$ where i and $j = 1,2,3$, t is time, and M, M') denote points of subsystem 1 and subsystem 2, respectively. According to the dual modal formulation, subsystem 1 is described by modes of the uncoupled-free subsystem (null stresses on $S_{Coupling}$) and subsystem 2 by modes of the uncoupled-blocked subsystem (null displacements on $S_{Coupling}$). (see Fig. 2).

Expanding displacements of subsystem 1 and stresses of subsystem 2, and assuming responses controlled by resonant contributions, gives

$$W_i(M, t) = \sum_{n=1}^{N_1} a_n(t)\tilde{W}_i^n(M), \tag{1}$$

$$\sigma_{ij}(M', t) = \sum_{s=1}^{N_2} b_s(t)\tilde{\sigma}_{ij}^s(M'), \tag{2}$$

where: $a_n(t)$, $b_s(t)$ are modal amplitudes for subsystem 1 and subsystem 2, respectively; $\tilde{W}_i^n(M)$ are displacement mode shapes of subsystem 1; $\tilde{\sigma}_{ij}^s(M')$ are stress mode shapes of subsystem 2; and N_1, N_2 are the number of resonant modes of subsystem 1 and subsystem 2, respectively.

With the change of modal variable,

$$b_q(t) = \dot{c}_q(t), \tag{3}$$

the modal equations given by the dual modal formulation (see Ref. [1]) are

$$\ddot{a}_p(t) + \Delta_p\dot{a}_p(t) + (\omega_p)^2 a_p(t) + \frac{1}{M_p}\sum_{m=1}^{N_2}\dot{c}_m(t)\mathbf{W}_{pm} = \frac{F_p}{M_p}, \quad \forall p \in [1, \ldots, N_1], \tag{4}$$

$$\ddot{c}_q(t) + \Delta_q\dot{c}_q(t) + (\omega_q)^2 c_q(t) - \frac{1}{(\omega_q)^2 M_q}\sum_{r=1}^{N_1}\dot{a}_r(t)\mathbf{W}_{rq} = \frac{F_q}{(\omega_q)^2 M_q}, \quad \forall q \in [1, \ldots, N_2], \tag{5}$$

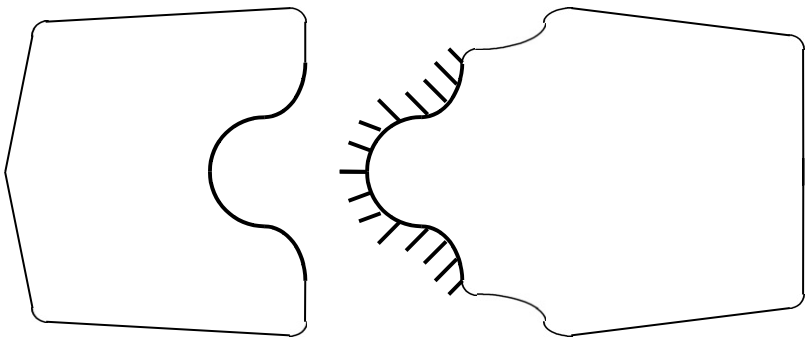

(a) (b)

Fig. 2. Representation of the uncoupled subsystems: (a) uncoupled-free subsystem 1; (b) Uncoupled-blocked subsystem 2.

where: Δ_p, Δ_q are modal damping bandwidths of each subsystem; ω_p, ω_q are natural angular frequencies of uncoupled subsystems; M_p, M_q are modal masses; F_p, F_q are generalized modal forces; and $\mathbf{W}_{pq}$ are interaction modal works yielded for each couple of modes (p,q) by

$$\mathbf{W}_{pq} = \int_{S_{Coupling}} \tilde{W}_i^p \, \tilde{\sigma}_{ij}^q \, n_j^2 \, \mathrm{d}S \tag{6}$$

and n_j^2 are components of the outer normal vector of the volume occupied by subsystem 2.

This system of equations describes the forced response of the coupled subsystems from the amplitudes of modes of the uncoupled subsystems.

The form of these equations allows us to interpret modes interactions as oscillators with gyroscopic couplings (see Fig. 3). Note that a mode of one subsystem is coupled to the modes of the other subsystem but is not directly coupled with the other modes of the subsystem to which it belongs. This configuration of mode coupling is exactly the one that supposes SEA.

3. Reformulation of SEA model without equipartition assumption

This section aims to reformulate the SEA model without taking into account equipartition of energy.

3.1. Modal energy equations

Consider mode p of subsystem 1. Its equation of motion is given in Eq. (4). The principle of conservation of energy applied to this mode gives

$$\Pi_{inj}^p = \Pi_{diss}^p + \sum_{q=1}^{N_2} \Pi_{pq}, \quad \forall p \in [1, \ldots, N_1], \tag{7}$$

where Π_{inj}^p is time-averaged injected power by the generalized force F_p; Π_{diss}^p is time-averaged dissipated power by internal damping of mode p; and $\sum_{q=1}^{N_2} \Pi_{pq}$ is time-averaged power flow exchanged by mode p with the modes of subsystem 2.

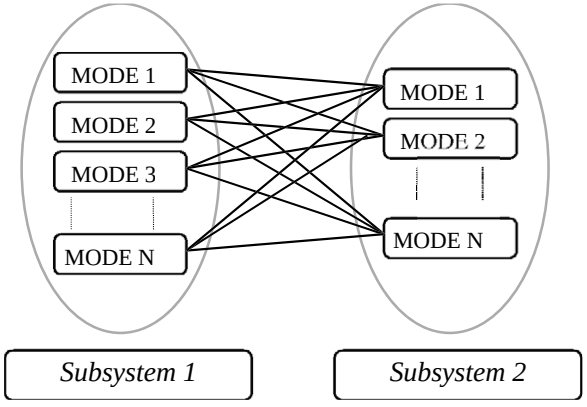

Fig. 3. Illustration of the interaction between N_1 modes of subsystem 1 and N_2 modes of subsystem 2.

The injected power into mode p by external excitation is either dissipated by internal damping of the mode or exchanged with modes of subsystem 2. The different powers appearing in this equation are estimated as follows:

Evaluating Π_{inj}^{p} from the power injected relation established for an oscillator excited by a white noise force [2] gives

$$\Pi_{inj}^{p} = \frac{\pi}{4M_p}\bar{S}_{F_p}, \tag{8}$$

where $\bar{S}_{F_p}$ is the power spectral density of the generalized force expressed in $N^2/rad/s$.

The power dissipated by internal damping of an oscillator (see Ref. [5]) can be related to its total energy by:

$$\Pi_{diss}^{p} = \omega_p \eta_p E_p, \tag{9}$$

where E_p is the time-averaged energy of mode p, and η_p is the modal damping factor ($\Delta_p = \omega_p \eta_p$).

To evaluate the power exchanged by mode p of subsystem 1 with mode q of subsystem 2, these two modes are isolated in the modal equations of motion (4) and (5):

$$\ddot{a}_p(t) + \Delta_p \dot{a}_p(t) + (\omega_p)^2 a_p(t) + \sqrt{\frac{(\omega_p)^2 M_q}{M_p}}\gamma_{pq}\dot{c}_q(t) = L_{1pq}(t), \quad \forall (p,\, q) \in ([1, N_1],\, [1, N_2]), \tag{10}$$

$$\ddot{c}_q(t) + \Delta_q \dot{c}_q(t) + (\omega_q)^2 c_q(t) - \sqrt{\frac{M_p}{(\omega_q)^2 M_q}}\gamma_{pq}\dot{a}_p(t) = L_{2qp}(t), \tag{11}$$

where

$$L_{1pq}(t) = \frac{F_p(t)}{M_p} - \sum_{\substack{r=1 \\ r\neq q}}^{N_2} \frac{\mathbf{W}_{pr}}{M_p}\dot{c}_r(t) \quad L_{2qp}(t) = \frac{F_q(t)}{(\omega_q)^2 M_q} + \sum_{\substack{m=1 \\ m\neq p}}^{N_1} \frac{\mathbf{W}_{mq}}{(\omega_q)^2 M_q}\dot{a}_m(t)$$

and

$$\gamma_{pq} = \frac{\mathbf{W}_{pq}}{\sqrt{M_p (\omega_q)^2 M_q}}.$$

Supposing, as classically done in SEA, that the interaction forces $L_{1pq}(t)$ and $L_{2qp}(t)$ are uncorrelated white-noise forces, the basic SEA relation established by Scharton and Lyon [30] can be used:

$$\Pi_{pq} = \omega_c \eta_{pq}(E_p - E_q), \tag{12}$$

where ω_c is the central angular frequency of the band of interest, and η_{pq} is called the modal coupling loss factor (see Ref. [1]). It is a function of natural angular frequencies, ω_p, ω_q; modal masses, M_p, M_q; modal bandwidths, Δ_p, Δ_q; and interaction modal works, $\mathbf{W}_{pq}$:

$$\eta_{pq} = \frac{(\mathbf{W}_{pq})^2}{\omega_c M_p (\omega_q)^2 M_q}\left(\frac{(\Delta_p(\omega_q)^2 + \Delta_q(\omega_p)^2)}{((\omega_p)^2 - (\omega_q)^2)^2 + (\Delta_p + \Delta_q)(\Delta_p(\omega_q)^2 + \Delta_q(\omega_p)^2)}\right). \tag{13}$$

Introducing Eqs. (8), (9), and (12) into Eq. (7), gives the power balance Eq. (14) for mode p of subsystem 1:

$$\Pi_{inj}^{p} = \omega_p \eta_p E_p + \sum_{q=1}^{N_2} \omega_c \eta_{pq}(E_p - E_q), \quad \forall p \in [1, \ldots, N_1]. \tag{14}$$

In the same way, energy balance equation of mode q of subsystem 2 can be written as

$$\Pi_{inj}^{p} = \omega_p \eta_p E_p + \sum_{p=1}^{N_2} \omega_c \eta_{pq}(E_p - E_q), \quad \forall q \in [1, \ldots, N_2]. \tag{15}$$

Relations (14) and (15) constitute a linear system of modal energies of subsystems 1 and 2:

$$\begin{aligned} \Pi_{inj}^{p} &= \left(\omega_p \eta_p + \sum_{q=1}^{N_2} \omega_c \eta_{pq}\right) E_p, - \sum_{q=1}^{N_2} \omega_c \eta_{pq} E_q, \quad \forall p \in [1, \ldots, N_1], \\ \Pi_{inj}^{q} &= - \sum_{p=1}^{N_1} \omega_c \eta_{pq} E_p + \left(\omega_q \eta_q + \sum_{p=1}^{N_1} \omega_c \eta_{pq}\right) E_q, \quad \forall q \in [1, \ldots, N_2]. \end{aligned} \tag{16}$$

The total energy of each subsystem can be finally obtained by adding modal energies

$$E_1 = \sum_{p=1}^{N_1} E_p, \qquad E_2 = \sum_{q=1}^{N_2} E_q, \tag{17}$$

where E_1 and E_2 are the time-averaged total energies of subsystem 1 and 2 respectively.

The model attached to the modal energy equations (16) is called SmEdA. The application of this model is not limited to theoretical structures, but can be applied to complex structures by using finite element method (FEM). As described in Refs. [1,31] to evaluate CLFs, FEM can be used to calculate the uncoupled subsystem modes which allow the modal coupling loss factors to be determined.

In the next Section, the link between SmEdA and SEA will be established.

3.2. Relations between SEA and SmEdA

In classical SEA, modal energy equipartition is assumed and allows the N_1 degree of freedom (d.o.f.) of subsystem 1 and the N_2 d.o.f. of subsystem 2 to be restricted to only two d.o.f., one per subsystem. Introducing equipartition relation (18),

$$\begin{aligned} E_p &= \frac{E_1}{N_1}, \quad \forall p \in [1, N_1], \\ E_q &= \frac{E_2}{N_2}, \quad \forall q \in [1, N_2], \end{aligned} \tag{18}$$

in the modal energy equations (16) and adding for each subsystem, mode energy balance equations, gives the standard SEA equation (19):

$$\Pi^1_{inj} = \omega_c \eta_1 E_1 + \omega_c \eta_{12} \left(E_1 - \frac{N_1}{N_2} E_2 \right),$$
$$\Pi^2_{inj} = \omega_c \eta_2 E_2 + \omega_c \eta_{12} \left(\frac{N_1}{N_2} E_2 - E_1 \right), \tag{19}$$

where $\Pi^1_{inj} = \sum_{p=1}^{N_1} \Pi^p_{inj}$ (resp. $\Pi^2_{inj} = \sum_{q=1}^{N_2} \Pi^q_{inj}$) represents the power injected by external sources in subsystem 1 (resp. subsystem 2), and, η_{12} is the SEA coupling loss factor given by

$$\eta_{12} = \frac{1}{N_1} \sum_{p=1}^{N_1} \sum_{q=1}^{N_2} \eta_{pq}. \tag{20}$$

In some practical applications, the equipartition assumption can be fulfilled by some subsystems but not by the others. In these situations, it will be interesting to mix SEA and SmEdA, classical SEA being used for subsystems where equipartition is valid and SmEdA for the others. To examine this point, consider the case of two subsystems, and assume equipartition is valid for subsystem 1 and not for subsystem 2; Eq. (16) becomes:

$$\Pi^1_{inj} = \omega_c (\eta_1 + \eta_{12}) E_1 \quad - \omega_c \sum_{q=1}^{N_2} \left(\sum_{p=1}^{N_1} \eta_{pq} \right) E_q, \tag{21}$$

$$\Pi^q_{inj} = -\frac{\omega_c}{N_1} \left(\sum_{p=1}^{N_1} \eta_{pq} \right) E_1 + \left(\omega_q \eta_q + \omega_c \sum_{p=1}^{N_1} \eta_{pq} \right) E_q, \quad \forall q \in [1, \ \ldots, \ N_2]. \tag{22}$$

The unknowns of these equations are the total energy of subsystem 1 and the N_2 modal energies of subsystem 2. It is thus possible to apply SmEdA only for the subsystem where equipartition is not achieved, and to use classical SEA for the other subsystem (application to four coupled plates is proposed in Ref. [32]).

4. Some examples

Three typical cases where equipartition is not achieved are shown in this Section: (a) coupling of subsystems with low modal overlap; (b) coupling of heterogeneous subsystems; (c) the case of localized excitation.

The following examples are based on beam and plate couplings in order to simplify the calculation. However, it should not be seen as limiting the approach; the application to complicated subsystems could be achieved, thanks to finite element models, in a straight forward manner.

In the following SmEdA denotes the present approach; SEA^{DMF} denote the SEA approach considering CLFs estimated by Eq. (13), i.e., the dual modal formulation; and SEA^{wave} denotes the SEA approach considering CLFs estimated by the classical wave approach (see Ref. [3]).

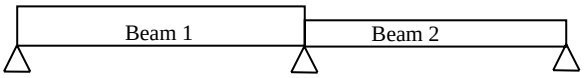

Fig. 4. Illustration of the rigid-coupled beams.

4.1. Coupling of subsystems with low modal overlap

4.1.1. Two subsystems

Two pinned–pinned beams coupled rigidly at one end, as shown in Fig. 4, are considered. L_α, b_α, h_α, E_α, ρ_α are, respectively, length, width, thickness, Young's modulus, and mass density of beam α. The subsystem boundary conditions are simply supported at both ends for beam 1 and clamped simply supported for beam 2. Rigid coupling is assumed (that is to say continuity of angular rotations and flexural moments) and thus the interaction modal works $\mathbf{W}_{pq}$ are expressed by

$$\mathbf{W}_{pq} = \tilde{\theta}_z^p \tilde{\mathbf{M}}_f^q, \tag{23}$$

where: $\tilde{\theta}_z^p$ is the pth mode angular rotation at the junction for beam 1, and $\tilde{\mathbf{M}}_f^q$ is the qth mode bending moment at the junction for beam 2.

In the following, only beam 1 is excited in the normalized octave band of central frequency 1000 Hz. The driving force is of a 'rain on the roof' type, and thus, power spectral densities of generalized forces (see Eq. (8)) are constant whatever the modes. In order to compare with classical calculations, solution based on wave decomposition for pure tone excitation was used, then frequency averaging of energy was done. Lastly, to approximate to rain on the roof excitation, beam energies obtained for 20 excitation points randomly distributed over beam 1 were averaged.

Beam lengths were chosen to have sufficient modes resonant in the excited band (10 modes for beam 1 and nine modes for beam 2).

Fig. 5 shows beam energies ratio E_2/E_1 versus geometric mean modal overlap. The geometric mean modal overlap factor $\bar{M}$ is given by

$$\bar{M} = \sqrt{M_1 M_2}, \tag{24}$$

where: M_α is beam α modal overlap: $M_\alpha = \omega_c \eta_\alpha n_\alpha, \alpha \in [1, 2]$; ω_c is the central angular frequency of the excited beam; η_α is the damping loss factor, and n_α is the modal density of beam α (see Ref. [3]).

SmEdA results agree with classical calculation for any geometric mean modal overlap whereas $\mathrm{SEA}^{\mathrm{DMF}}$ gives poor estimates when $\bar{M} < 0.1$. It can also be seen that $\mathrm{SEA}^{\mathrm{wave}}$ gives approximately the same results as $\mathrm{SEA}^{\mathrm{DMF}}$.

The poor prediction of $\mathrm{SEA}^{\mathrm{DMF}}$ suggests that equipartition is not achieved when modal overlap is weak. This point is confirmed in Fig. 6 where the distribution of modal energies of the non-excited beam is presented for four different values of the geometric mean modal overlap. For the highest value, equipartition is quite fulfilled explaining that $\mathrm{SEA}^{\mathrm{DMF}}$ gives good results. For the lowest value (Fig. 6(a)), there is a large disparity between modal energies: the fourth mode in the frequency band considered largely dominates the response. In this case, $\mathrm{SEA}^{\mathrm{DMF}}$ gives poor results. However, strong disparities of modal energies do not lead systematically to a poor estimation of energies by SEA. Comparing Figs. 6(a) and (b), disparities of modal energies are

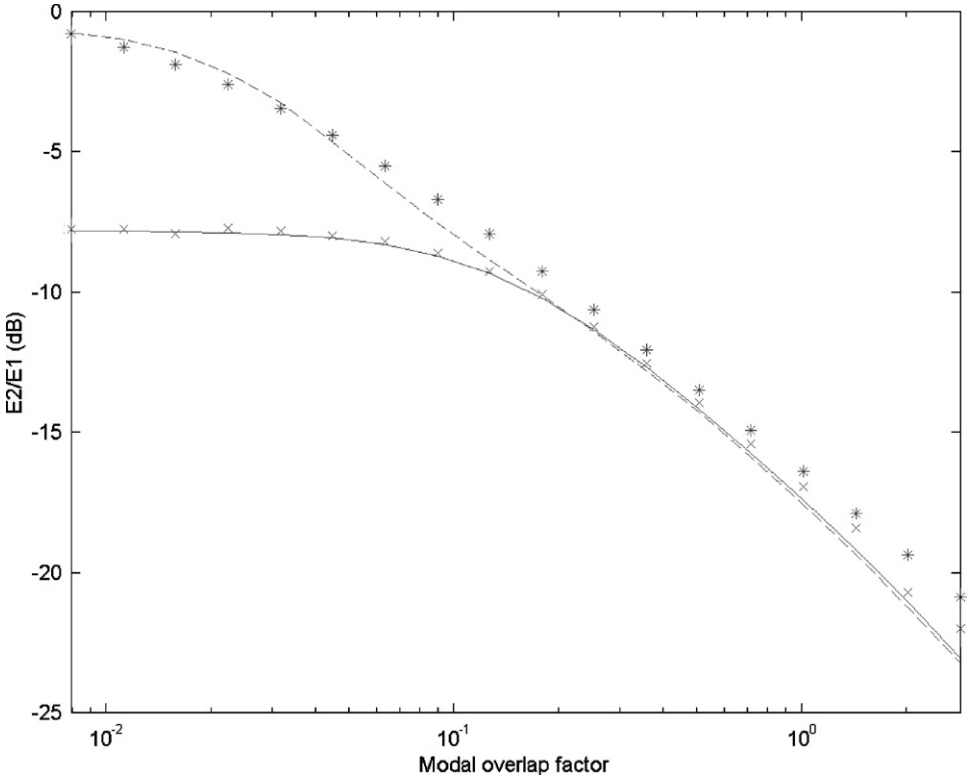

Fig. 5. Beam energy ratio, E_2/E_1, versus the geometric mean of the modal overlap factors, $\sqrt{M_1 M_2}$ (octave band 1000 hz). Comparison of four calculations: x, exact; —, SmEdA; —, $\mathrm{SEA}^{\mathrm{DMF}}$; *, $\mathrm{SEA}^{\mathrm{wave}}$. $L_1 = 2.4$ m, $L_2 = 1.2$ m, $b_1 = b_2 = 0.01$ m, $h_1 = 3$ mm, $h_2 = 1$ mm, $E_1 = E_2 = 7 \times 10^{10}$ Pa, $\rho_1 = \rho_2 = 2700\,\mathrm{kg/m^3}$, $N_1 = 10$ modes, $N_2 = 9$ modes.

similar but SEA results are very different in the two cases: through the middle in (b), but through the peak in (a). In case (a), SEA overestimates largely energy transfer; whereas in case (b), SEA prediction is reasonably good (see Fig. 5).

Modal energy disparities are due to frequency coincidence that has a significant role in the modal couplings when modal overlap factors are less than one (see expression (13)); some modes can be strongly coupled whereas other ones are much less. Fig. 7 shows where modal coupling loss factors are plotted. When damping is low (Fig. 7(a)), the coupling between the two beams are dominated by the interaction between the fourth mode of beam 1 and the fourth mode of beam 2 (due to close natural frequencies); then equipartition is not achieved (see Fig. 6(a)). On the other hand, when the mean geometric modal overlap factor is equal or greater than one (see Figs. 7 (c) and (d)), all modes of beam 2 are strongly coupled to at least one mode of beam 1, and in this case equipartition is achieved (see Fig. 6 (c) and (d)).

Several studies [7,12,14,29] have shown, as can be seen here, that classical SEA overestimates the energy transfer between subsystems when modal overlap factors are much less than one. The present results demonstrate that, in this case, modal equipartition is not fulfilled and is responsible of the poor prediction of SEA. This was previously mentioned in Ref. [7].

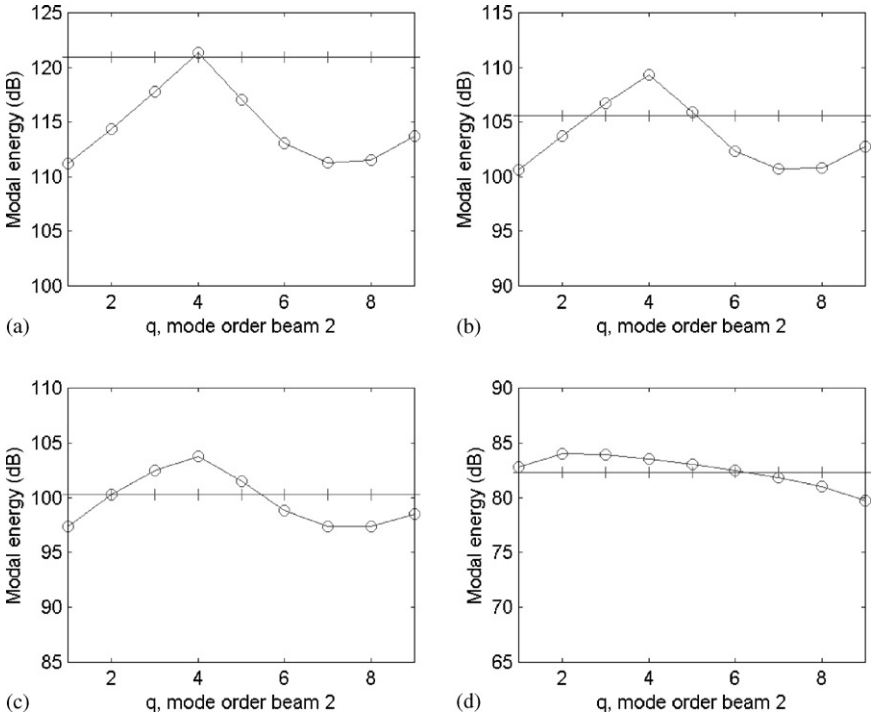

Fig. 6. Modal energy distribution of the receiving beam (dB, ref. 10^{-12} joule). Resonant modes classified with increasing natural frequencies. Four cases: (a) $\bar{M} = 7.9 \times 10^{-3}$; (b) $\bar{M} = 0.09$; (c) $\bar{M} = 0.18$; (d) $\bar{M} = 1.43$. Two calculations: -o-o-, SmEdA; $\bar{+}$, $\mathrm{SEA}^{\mathrm{DMF}}$.

The γ factor was proposed separately by Mace [16] and Finnveden [17] as an indicator of the coupling strength of two subsystems. When γ is much less than one, the coupling between two subsystems is called weak, i.e. classical SEA is valid and

$$\gamma = \frac{\tau_{12}}{2\pi^2 M_1 M_2}, \tag{25}$$

where τ_{12} is the transmission factor.

Table 1 presents the γ factor (25) for different cases treated in Fig. 5. It can be observed that this criterion confirms the validity of SEA; namely when $\gamma > 1$, $\mathrm{SEA}^{\mathrm{wave}}$ fails, but SmEdA still allows the energy flow to be predicted and appears to be alternative to SEA for strong coupling.

Another example based on plate coupling was presented in Ref. [2]. Because the coupling effects are distributed along a line, spatial coincidence of mode shapes has a significant role and can lead several modes of the non-excited subsystem to be uncoupled from modes of the excited subsystem. This increases the disparity of the distribution of modal energies, SEA can then overestimate energy transfer even if geometric mean modal overlap is equal or greater than one, whereas SmEdA gives good results.

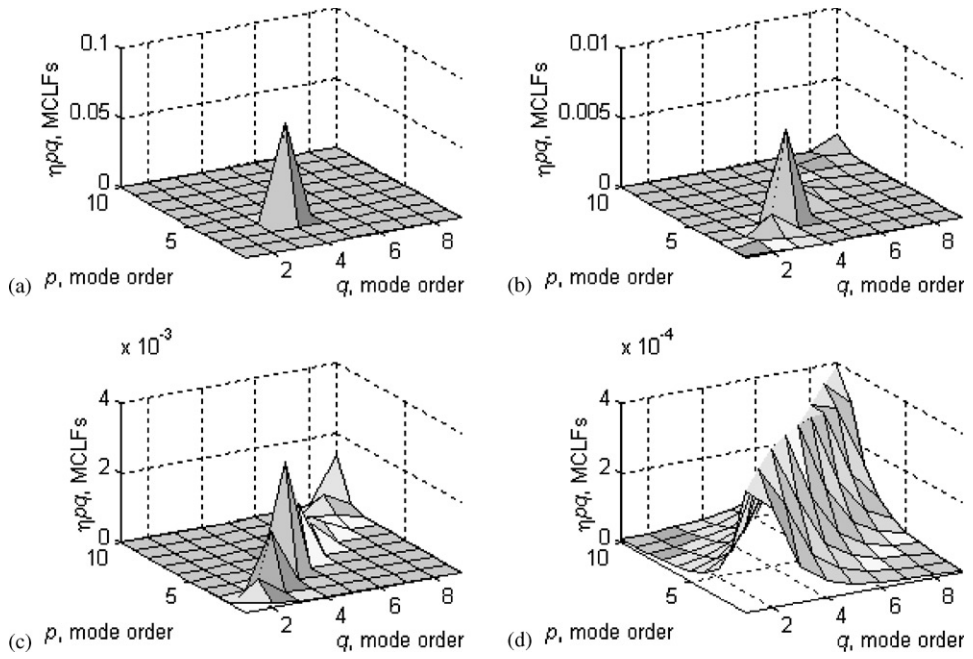

Fig. 7. Modal coupling loss factors, η_{pq}. (Modes classified with increasing natural frequencies.) Same cases than the previous figure: (a) $\bar{M} = 7.9 \times 10^{-3}$; (b) $\bar{M} = 0.09$; (c) $\bar{M} = 0.18$; (d) $\bar{M} = 1.43$.

Table 1
$\bar{M}$, geometric mean modal overlap factor; η, damping loss factor; γ, gamma factor. Values for different cases of Fig. 5

$\bar{M}$	0.0079	0.016	0.032	0.063	0.127	0.254	0.508	1.016	2.032
η	0.0005	0.001	0.002	0.004	0.008	0.016	0.032	0.064	0.128
γ	91.1	22.77	5.69	1.42	0.35	0.09	0.02	0.01	0.002

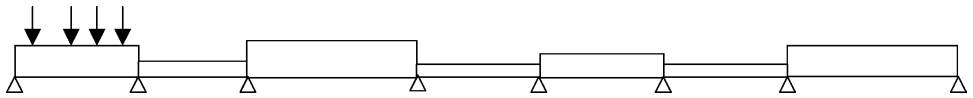

Fig. 8. Schematic representation of the seven rigidly coupled beams. Rain on the roof excitation on beam 1. $L_1 = 2.4$ m, $L_2 = 1.2$ m, $L_3 = 2.2$ m, $L_4 = 1.4$ m, $L_5 = 2$ m, $L_6 = 1.2$ m, $L_7 = 2.3$ m, $h_1 = 3$ mm, $h_2 = 1$ mm, $h_3 = 4$ mm, $h_4 = 1.2$ mm, $h_5 = 2$ mm, $h_6 = 0.8$ mm, $h_7 = 3.5$ mm, $b_\alpha = 0.01$ m, $E_\alpha = 7 \times 10^{10}$ Pa, $\rho_\alpha = 2700$ kg/m^3, $\eta_\alpha = 0.001$ ($\alpha \in [1,7]$).

4.1.2. *Multiple subsystems*

Now, consider a structure composed of seven pinned–pinned beams coupled rigidly in a chain as shown Fig. 8. At each junction, simple supports are introduced in order to simplify subsystems modes calculations. This also produces very large overall attenuation that demonstrates clearly the difference of predictions between SEA and SmEdA.

In the following, rain on the roof excitation is applied on beam 1 and each beam has a damping loss factor of 0.1% ($\eta = 0.001$); that is to say the modal overlap factor is less than unity (geometric mean modal overlap factor, $\bar{M} = 0.0125$).

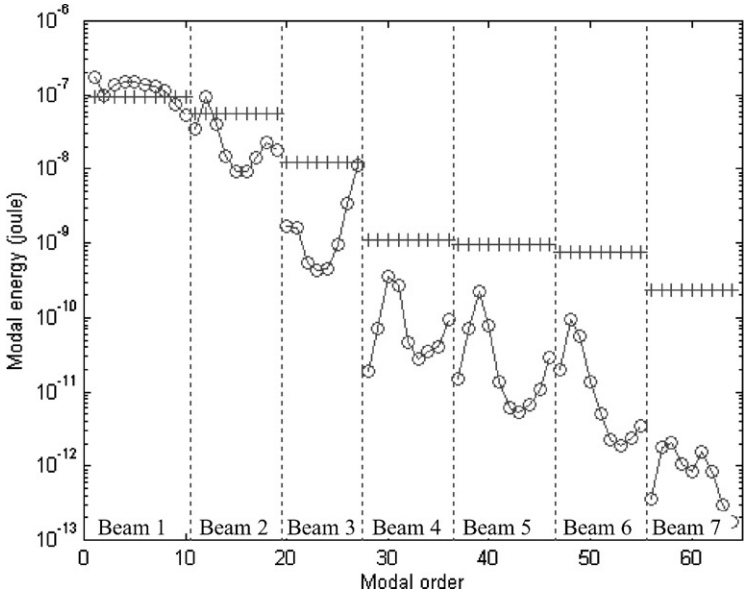

Fig. 9. Modal energy distributions of the seven beams in the case of weak modal overlap: $\eta_\alpha = 0.001$ ($\alpha \in [1,7]$). Octave band of central frequency 1000 Hz. Two calculations: -o-o-, SmEdA; $\bar{+}$, $\mathrm{SEA}^{\mathrm{DMF}}$.

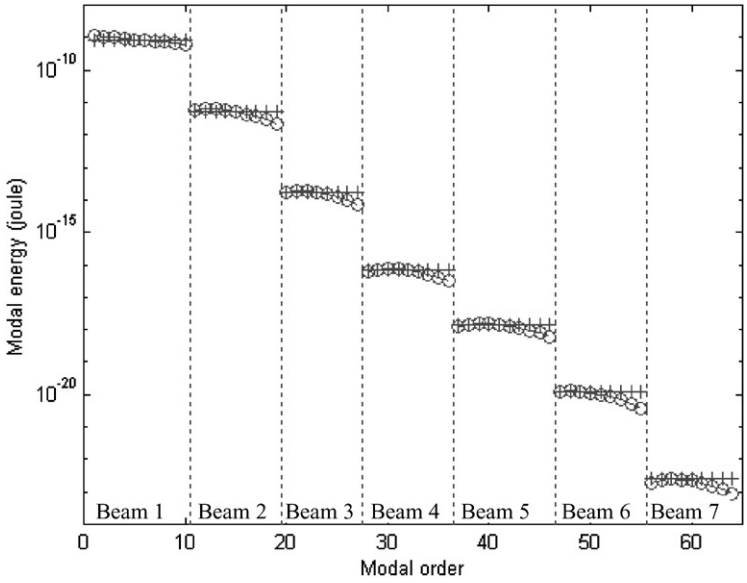

Fig. 10. Modal energy distributions of the seven beams in the case of geometric mean modal overlap factors equal to one (octave band of central frequency 1000 Hz). Two calculations: -o-o-, SmEdA; $\bar{+}$, $\mathrm{SEA}^{\mathrm{DMF}}$.

The SmEdA model has been constructed when this structure is decomposed into seven subsystems. The boundary conditions used to extract the uncoupled subsystems modes are clamped–clamped for beams 2, 4 and 6 (blocked subsystems), and pinned–pinned for beams 1, 3, 5 and 7 (free subsystems).

Fig. 9 presents modal energies distributions in beams. The main tendency that appears is an increase of beam modal energies disparities, subsystem after subsystem. Then, the equipartition assumption lead to gross overestimates of energy transmission far from the excited beam (see also Ref. [7]).

The disparities come from resonance frequency coincidences that render one modal interaction dominant. Of course, the probability of having the phenomena increases with the number of coupled subsystems. In the case of high modal overlap, this effect no longer has a significant role and as shown in Fig. 10 equipartition of modal energy is achieved.

4.2. Heterogeneous subsystems

Classical SEA assumes a vibratory diffuse wave field in each subsystem [19], when SEA substructuring should be used. However, for industrial structures such as panel stiffened by spars and stringers, it is not possible to have a diffuse field because of heterogeneity. The assumption of the diffuse field of the wave approach can be related to the equipartition assumption of the modal approach. Because SmEdA does not assume equipartition, one can expect it can be used for heterogeneous structures. To make this point clear four Euler–Bernoulli beams coupled rigidly at each end with an intermediary support (see Fig. 11) are studied. The external ends are simply supported for beam 1 and clamped for beam 4. Beam 1 is excited by rain 'on the roof' excitation.

The substructuring which is considered is shown in Fig. 11: beams 1 and 4 are independant subsystems (subsystems 1 and 3, respectively), whereas beams 2 and 3 constitute a single non-homogeneous subsystem (subsystem 2).

Although analytic modal extraction can be performed, the finite elements method was used to calculate the modal information of each subsystem. Modal coupling loss factors are obtained by the technique used in Ref. [1] to calculate coupling loss factors from FEM data. The modal information for each mode is eigenfrequency, generalized mass and mode shape at the coupling ends in terms of nodal displacement for free junctions and of nodal force for blocked junctions. Expression (80) of Ref. [1] is used to calculate interaction modal works, and then Eq. (13) used to calculate modal coupling loss factors.

For the octave band of central frequency 1000 Hz, the energy ratio between the receiving beam 4 and the excited beam 1 is equal to −36.3 dB using SmEdA and −24.0 dB using SEA whereas a reference energy ratio obtained by FE numerical experiments (see Ref. [31]) is −38.3 dB. SEA

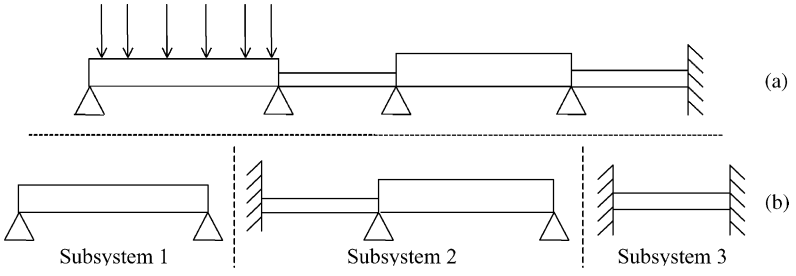

Fig. 11. (a) Illustration of the four coupled beams; (b) Substructuring. Beams' characteristics: $L_1 = 2.4\,\text{m}$, $L_2 = 1.2\,\text{m}$, $L_3 = 2.2\,\text{m}$, $L_4 = 1.4\,\text{m}$, $h_1 = 3\,\text{mm}$, $h_2 = 1\,\text{mm}$, $h_3 = 5\,\text{mm}$, $h_4 = 1.2\,\text{mm}$, $b_\alpha = 0.01\,\text{m}$, $E_\alpha = 7 \times 10^{10}\,\text{Pa}$, $\rho_\alpha = 2700\,\text{kg/m}^3$, $\eta_\alpha = 0.01$ ($\alpha \in [1,4]$).

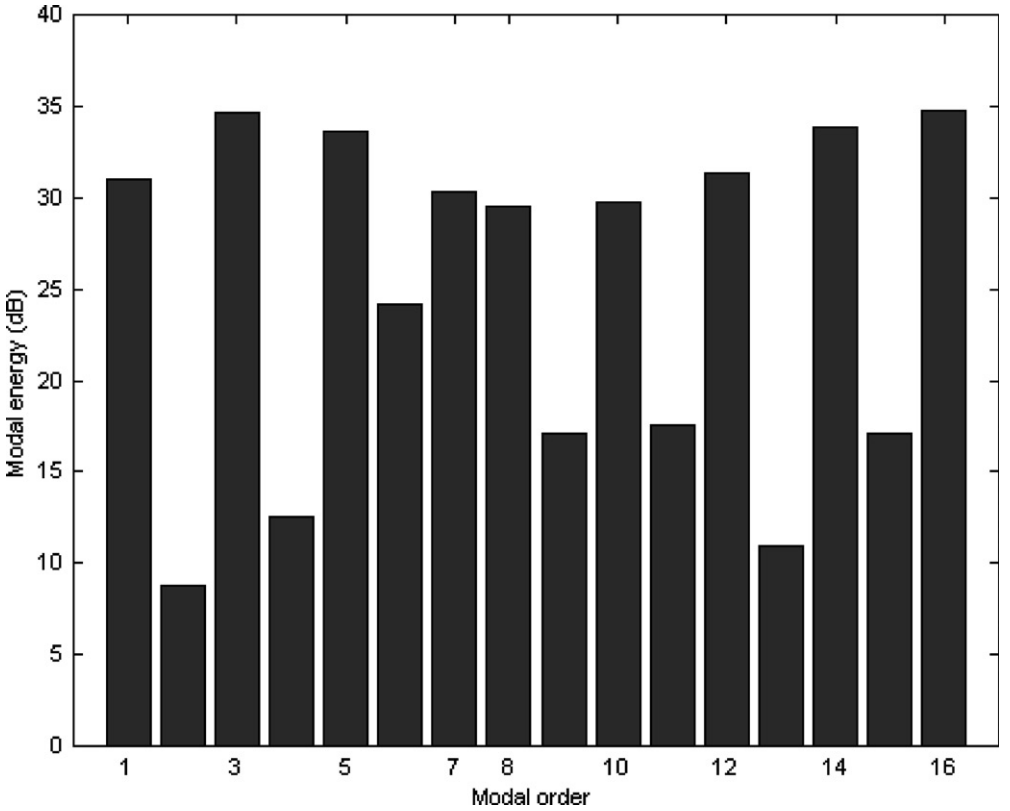

Fig. 12. Modal energy distribution of subsystem 2 (dB, ref. 10^{-12} joule) . Modes classified with increasing natural frequencies. SmEdA results.

gives an error of 14.3 ds whereas SmEdA gives an accurate prediction. This can be explained again by observing the modal energies distribution of subsystem 2 (Fig. 12) where important variations can be seen on the modal distribution. SEA is not able to describe these variations, and it overestimates the energy transfer between subsystems 2 and 3. The heterogeneity of subsystem 2 produces local modes, as illustrated in Fig. 13. The mode shapes act on the modal coupling loss factors via the interaction modal factors. The difference of mode shape amplitudes at each end of the subsystem implies that the mode is lightly coupled with modes of the right subsystem and strongly coupled with those of the left subsystem (or vice versa). This introduces a strong disparity of mode energies which can only be taken into account by considering each mode independently. This explains why SEA fails and SmEdA gives good results. In this specific demonstration case, it can be argued, however, that intuitively, one would actually choose four SEA elements for the analysis, and such a choice would give similar good agreement for beam 4, namely −34.3 dB.

4.3. *Case of localized excitation*

In Sections 4.1 and 4.2, the external sources were of the rain on the roof type. This excitation is considered in SEA because it produces decorrelation of generalized forces and thus modal

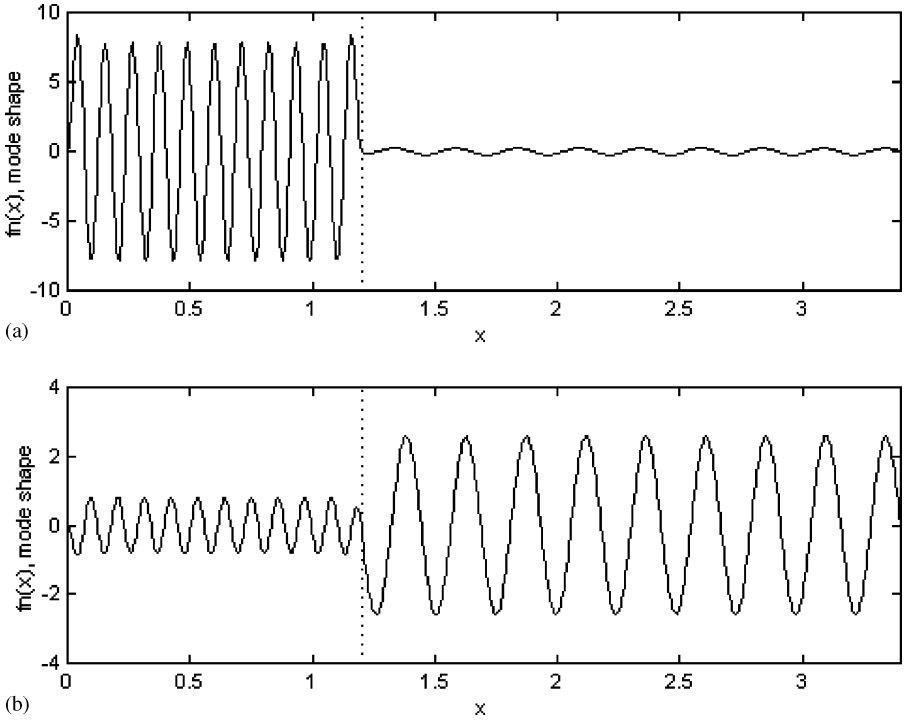

Fig. 13. Examples of displacement mode shapes for subsystem 2: (a) mode 1 of the previous figure; (b) mode 2 of the previous figure.

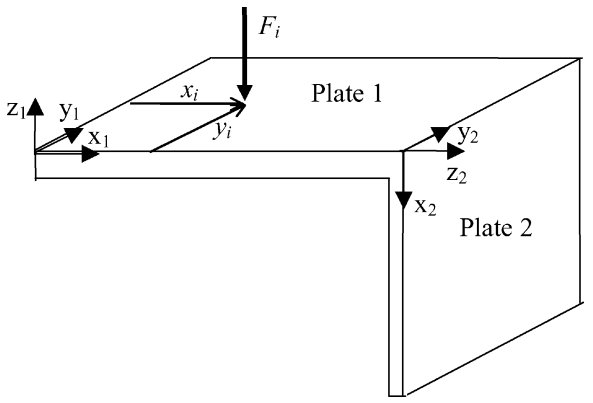

Fig. 14. Two plates coupled in an L-shape and excited by a point force F_i on plate 1: $a_1 = 1.7$ m, $a_2 = 0.8$ m, $b = 1$ m, $h_1 = 6$ mm, $h_2 = 3$ mm, $E_1 = E_2 = 2 \times 10^{11}$ Pa, $\rho_1 = \rho_2 = 7800$ kg/m^3, $\eta_1 = \eta_2 = 0.01$.

energies equipartition for the excited subsystem (see Ref. [23]). However, in practical situations, sources cannot always be assimilated to rain on the roof excitation, leading to difficulty in using SEA, unlike to SmEdA.

Consider two thin steel plates coupled in an L shape. Plate 1 is excited by one white-noise point force. Each plate is simply supported on non-coupled edges and flexural motions are considered (see Fig. 14).

Let plate 2 be thinner than plate 1. Then, according to DMF, plate 1 is described by free modes at junction and plate 2 by blocked modes. This modal information is given in Appendix A. The interaction modal work between mode (m,n) of plate 1 and mode (r,s) of plate 2 is

$$\mathbf{W}_{mn,rs} = \begin{cases} \dfrac{E_2 b h_2^3 \kappa_r}{12(1-\nu_2^2)} \left(\dfrac{m\pi}{a_1}\right) \left(\dfrac{s\pi}{b}\right)^2 \sin\left(\dfrac{s\pi}{b}\sqrt{\kappa_r+1}\right), & \text{if } n = s, \\ 0, & \text{if } n \neq s \end{cases} \tag{26}$$

Table 2
(x_i, y_i) co-ordinates of point excitation i

i	1	2	3	4	5	6	7	8	9	10	11	12
x_i (m)	0.65	0.14	1.11	0.96	0.50	1.30	0.36	1.49	1.26	0.30	0.84	1.50
y_i (m)	0.75	0.73	0.55	0.63	0.21	0.65	0.06	0.24	0.62	0.80	0.40	0.50

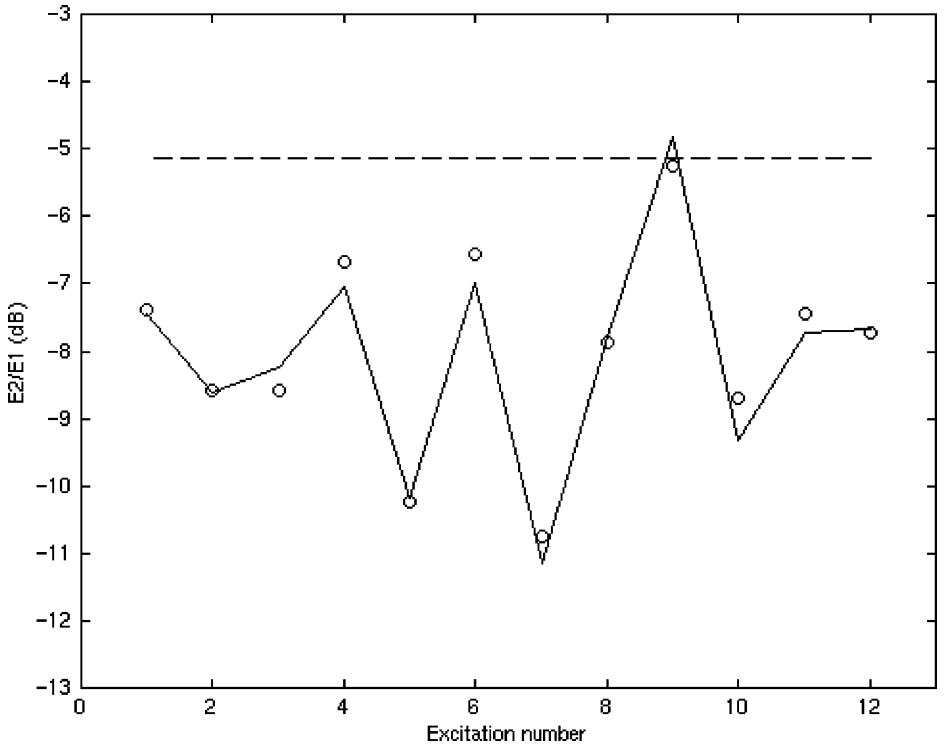

Fig. 15. Total energy ratio for each excitation point. Third octave band of central frequency 1000 Hz. Comparison of three calculations: o, reference obtained from DMF with non-resonant modes; —, SmEdA; - - - -, SEA.

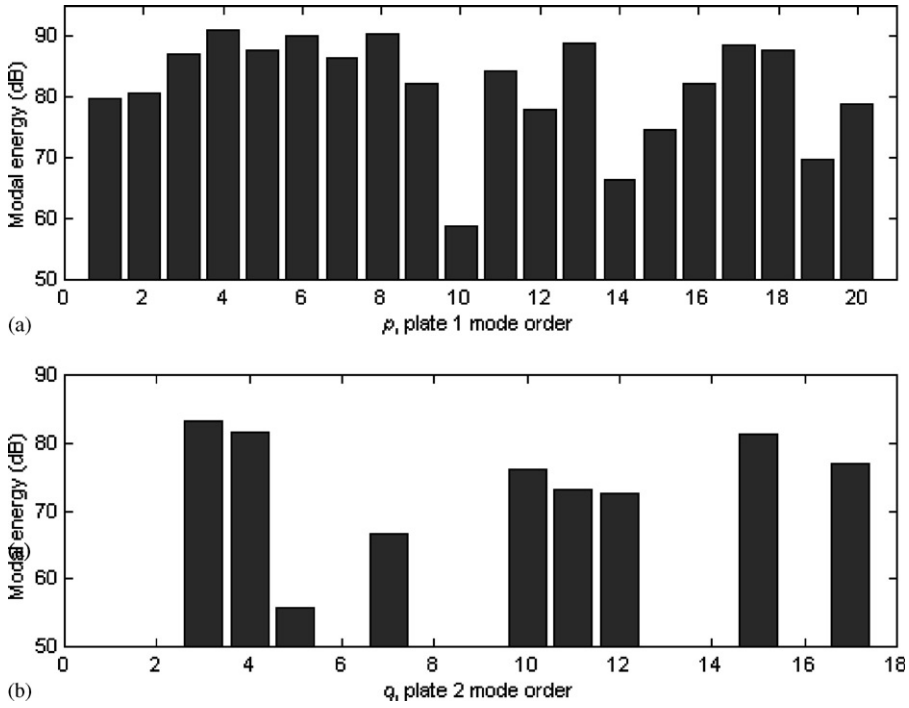

Fig. 16. Modal energy distributions for excitation case number 7 (dB, ref. 10^{-12} joule): (a) plate 1, (b) plate 2. Modes classified with increasing natural frequencies.

where: a_α, b, h_α, E_α, v_α are, respectively, longitudinal length, length of the common edge, thickness, Young modulus, and the Poisson ratio for plate α, $\alpha = 1, 2$; and κ_r is a modal parameter given in Appendix A.

It can be seen that the interaction modal work (26) is zero for pairs of modes which do not have the same index on the common edge ($n \neq s$).

The power injected by the driving force located at point (x_i, y_i) in mode (m,n) of plate 1 is

$$P_{inj}^{mn} = \frac{\pi S_f}{\rho_1 h_1 a_1 b}\left[\sin\left(\frac{m\pi}{a_1}x_i\right)\sin\left(\frac{n\pi}{b}y_i\right)\right]^2, \tag{27}$$

where S_f is the power spectral density of force for the frequency band of interest ($N^2/(rad/s)$), and ρ_1 is mass density of plate 1.

The modal injected power can vary strongly from one mode to another, contrary to the case of rain on the roof excitation.

SmEdA application used Eq. (27) to evaluate modal input power. Twelve different excitation positions were studied; their co-ordinates are given in Table 2. Fig. 15 shows the plates energies ratio, for excitation in the third octave band of centre frequency 1000 Hz. A good agreement can be seen between SmEdA and reference results (obtained by DMF calculation taking into account modes belonging to the octave band of centre frequency 1000 Hz). This is due to the variation of modal energies as is clearly demonstrated in Fig. 16. The variation of modal injected power introduced a variation of modal energy in the excited plate that was accentuated by a modal

coupling filtering effect for the modal energy distribution in plate 2: in the excited band, 20 resonant modes contribute to vibrations for plate 1 and 17 for plate 2, but due to null interaction modal work only nine modes of plate 2 are significantly excited.

5. Conclusions

This paper presents a reformulation of SEA taking modal energy distribution into account. The necessary data to build the model include modal information for each uncoupled subsystem: natural frequencies, modal masses, modal damping and mode shapes on the coupling boundaries. FEMs can be used to calculate modal information in the cases of complex subsystems that allow this technique to be applied to industrial structures. The results are given in terms of modal energies which can be added to calculate subsystem energies.

The use of the SmEdA techniques has been demonstrated on some simple examples.

The coupling of subsystems with low modal overlap factors which has been widely discussed in the literature can be solved by SmEdA. In this case, the modal energy distribution is non-uniform due to the effect of frequency and space coincidences.

Energies can be predicted by SmEdA for heterogeneous subsystems which are of great interest when dealing with industrial structures.

Localized excitation can lead to important variations in the modal energies distribution of the excited subsystem which cannot be described by classical SEA. A coupled plates example has shown that SmEdA can correctly predict the effect of source position.

Finally, SmEdA can easily be combined with classical SEA, in order to calculate energy distribution only in subsystems where it is necessary, and use SEA for others subsystems. To apply SEA to coupled subsystems necessitates that all subsystems verify SEA assumption. This is very restrictive for industrial practical application because some subsystems are highly heterogeneous, locally excited or have weak modal overlap. In this case, the coupling of SmEdA for these subsystems with SEA for others allows the problem is to be solved. Of course, the use of SmEdA necessitates the calculation of the uncoupled subsystem modes, but this is only required for these particular subsystems for which SmEdA is useful.

Acknowledgements

The authors are grateful for the interest and financial support of DGA/DSP Paris (Direction des Systèmes de forces et de Prospective) and DGA/CTSN Toulon (Centre Technique des Systèmes Navals), without which this work would have not been carried out.

Appendix A. Modal information for the L-shaped plates

The structure and the co-ordinate systems are shown in Fig. 14. In accordance with DMF, plate 1 is described by modes of the uncoupled - free subsystem and plate 2 by modes of the uncoupled-blocked subsystem. Thus, the modal information of plate 1 are obtained by considering the plate

simply supported on its four edges:

$$\omega_{mn} = \sqrt{\frac{h_1^2 E_1}{12(1-\nu_1^2)\rho_1}}\left(\left(\frac{m\pi}{a_1}\right)^2 + \left(\frac{n\pi}{b}\right)^2\right), \tag{A.1}$$

$$M_{mn} = \frac{\rho_1 h_1 a_1 b_1}{4}, \tag{A.2}$$

$$\tilde{W}^{mn}(x_1, y_1) = \sin\left(\frac{m\pi}{a_2}x_1\right)\sin\left(\frac{n\pi}{b}y_1\right), \tag{A.3}$$

and those of plate 2 by considering the plate clamped on the coupling edge $x_2 = 0$ and simply supported on the others edges (see the technique of calculation in Ref. [33, pp. 84–85]:

$$\omega_{rs} = \sqrt{\frac{h_2^2 E_2}{12(1-\nu_2^2)\rho_2}}\left(\frac{s\pi}{b}\right)^2 \kappa_r \text{ with } \kappa_r/\sqrt{\kappa_r - 1}\tanh\left(\frac{b}{a_2}s\pi\sqrt{\kappa_r + 1}\right) = \sqrt{\kappa_r + 1}\tanh\left(\frac{b}{a_2}s\pi\sqrt{\kappa_r - 1}\right),$$

$$M_{rs} = \int_0^{a_2}\int_0^{b} \rho_2 h_2 (\tilde{W}^{rs}(x_2, y_2))^2 \, \mathrm{d}y_2 \, \mathrm{d}x_2, \tag{A.4}$$

$$\begin{cases} \tilde{\sigma}_{xx}^{rs}(x_2, y_2) = -\dfrac{E_2}{1-\nu_2^2}\dfrac{\partial^2 \tilde{W}^{rs}}{\partial x_2^2}(x_2, y_2) - \dfrac{\nu_2 E_2}{1-\nu_2^2}\dfrac{\partial^2 \tilde{W}^{rs}}{\partial y_2^2}(x_2, y_2), \\ \tilde{\sigma}_{yy}^{rs}(x_2, y_2) = -\dfrac{\nu_2 E_2}{1-\nu_2^2}\dfrac{\partial^2 \tilde{W}^{rs}}{\partial x_2^2}(x_2, y_2) - \dfrac{E_2}{1-\nu_2^2}\dfrac{\partial^2 \tilde{W}^{rs}}{\partial y_2^2}(x_2, y_2), \\ \tilde{\sigma}_{xy}^{rs}(x_2, y_2) = -\dfrac{E_2}{1+\nu_2}\dfrac{\partial^2 \tilde{W}^{rs}}{\partial x_2 \partial y_2}(x_2, y_2) \end{cases} \tag{A.5}$$

with

$$\tilde{W}^{rs}(x_2, y_2) = \sin\left(\frac{s\pi}{b}y_2\right)\left[\sinh\left(\frac{s\pi\sqrt{\kappa_r + 1}}{b}(a_2 - x_2)\right) - \frac{\sinh\left(\dfrac{a_2 s\pi\sqrt{\kappa_r + 1}}{b}\right)}{\sin\left(\dfrac{a_2 s\pi\sqrt{\kappa_r - 1}}{b}\right)}\sin\left(\frac{s\pi\sqrt{\kappa_r - 1}}{b}(a_2 - x_2)\right)\right], \tag{A.6}$$

where $\tilde{W}^{mn}$ is the displacement mode shapes of plate 1 and $\tilde{\sigma}_{xx}^{rs}$, $\tilde{\sigma}_{yy}^{rs}$, $\tilde{\sigma}_{xy}^{rs}$ are the stress mode shapes of plate 2.

For the case of two plates coupled in an L-shape, the interaction modal work between the mode (m,n) of plate 1 and the modes (r,s) of plate 2 is given by

$$\mathbf{W}_{mn,rs} = \frac{b h_2^3}{12}\int_0^{b} \frac{\partial \tilde{W}^{mn}}{\partial x_1}(a_1, y)\tilde{\sigma}_{xx}^{rs}(0, y)\, \mathrm{d}y, \tag{A.7}$$

and can be rewritten by using the mode shapes (A.3), (A.6):

$$\mathbf{W}_{mn,rs} = \begin{cases} \dfrac{E_2 b h_2^3 \kappa_r}{12(1-\nu_2^2)} \left(\dfrac{m\pi}{a_1}\right) \left(\dfrac{s\pi}{b}\right)^2 \sin\left(\dfrac{s\pi}{b}\sqrt{\kappa_r+1}\right), & \text{if } n = s, \\ 0, & \text{if } n \neq s, \end{cases} \tag{A.8}$$

References

[1] L. Maxit, J.-L. Guyader, Estimation of SEA coupling loss factors using a dual formulation and FEM modal information Part 1: theory Part 2: numerical applications, Journal of Sound and Vibration 239 (2001) 907–948.

[2] L. Maxit, Extension et reformulation du modèle SEA par la prise en compte de la répartition des énergies modales, Ph.D.Thesis, Institut National des Sciences Appliquées de Lyon, France, 2000.

[3] R.H. Lyon, R.G. Dejong, Theory and Application of Statistical Energy Analysis, Butterworth, London, 1995.

[4] C.B. Burroughs, R.W. Fischer, F.R. Kern, An introduction to statistical energy analysis, The Journal of the Acoustical Society of America 101 (1997) 1779–1789.

[5] E.E. Ungar, Fundamentals of statistical energy analysis of vibrating systems, US Air Force AFFDL-TR 66–52, April, 1966.

[6] A.J. Kean, W.G. Price, Statistical energy analysis of strongly coupled systems, Journal of Sound and Vibration 117 (1987) 363–386.

[7] F.F. Yap, J. Woodhouse, Investigation of damping effects on statistical energy analysis of coupled structures, Journal of Sound and Vibration 197 (1996) 351–371.

[8] C. Fredo, Statistical Energy Analysis and the Individual Case, Ph.D.Thesis, Chalmers University of Technology, Sweden, 1995.

[9] S. Finnveden, Energy flows within a three element structure with statistical description of the design parameters, Internoise90, Gothenburg, Sweden, August, 1990.

[10] B.R. Mace, P.J. Shorter, Irregularity, damping, and coupling strength in sea, IUTAM Symposium on Statistical Energy Analysis, Southampton, UK, 8–11 July, 1997.

[11] B.R. Mace, J. Rosenberg, The sea of two coupled plates: an investigation into the effects of subsystem irregularity, Journal of Sound and Vibration 212 (1998) 395–415.

[12] R.S. Ming, J. Pan, The limitation in the sea prediction of power transmission and energy distribution, Fifth International Congress on Sound and Vibration, Adelaide, Australia, December, 1997.

[13] W.S. Park, D.J. Thompson, N.S. Ferguson, Sources of error and confidence intervals for SEA parameters, NOVEM Meeting, Lyon, France, September, 2000.

[14] F.J. Fahy, A.D. Mohammed, A study of uncertainty in applications of sea to coupled beam and plate systems, Part I: computational experiments, Journal of Sound and Vibration 158 (1992) 45–67.

[15] B.R. Mace, The statistical energy analysis of two continuous one-dimensional subsystems, Journal of Sound and Vibration 166 (1993) 429–461.

[16] B.R. Mace, On the statistical energy analysis hypothesis of coupling power proportionality and some implications of its failure, Journal of Sound and Vibration 178 (1994) 95–112.

[17] S. Finnveden, Ensemble averaged vibration energy flows in a three-element structure, Journal of Sound and Vibration 187 (1995) 495–529.

[18] S. Finnveden, Coupling strength criterion for the modal approach to statistical energy analysis of spring coupled elements, Internoise98, Christchurch, New Zealand, 16–18 November, 1998.

[19] R.S. Langley, A wave intensity technique for the analysis of high frequency vibration, Journal of Sound and Vibration 159 (1992) 485–502.

[20] R.S. Langley, A.N. Bercin, Wave intensity analysis of high frequency vibrations, Philosophical Transactions Royal Society London A346 (1994) 489–499.

[21] H. Nishino, M. Ohlrich, Prediction of medium frequency vibration by wave intensity analysis, NOVEM Meeting, Lyon, France, September, 2000.

[22] J.-G. Ih, K.S. Chae, Use of the ray tracing method for predicting the vibration energy distribution in the thin plate at high frequencies, NOVEM Meeting, Lyon, France, September, 2000.
[23] E.K. Dimitriadis, A.D. Pierce, Analytical solution for the power exchange between strongly coupled plates under random excitation: a test of statistical energy analysis concepts, Journal of Sound and Vibration 123 (1988) 397–412.
[24] C. Boisson, J.-L. Guyader, C. Lesueur, Étude numérique de la transmission d'énergie vibratoire entre structures assemblées: cas d'assemblages en L, T et +, Acustica 58 (1985) 223–233.
[25] G. Fortunato, K. De Langhe, The influence of boundary conditions on sea parameters in the low and high frequency range, Sixth International Congress on Sound and Vibration, Copenhagen, Denmark, 5–8 July, 1999.
[26] R.S. Langley, A general derivation of the statistical energy analysis equations for coupled dynamic systems, Journal of Sound and Vibration 135 (1989) 499–508.
[27] H.G. Davies, Random vibration of distributed systems strongly coupled at discrete points, The Journal of the Acoustical Society of America 54 (1973) 507–515.
[28] G. Maidanik, J. Dickey, Modal and wave approaches to the statistical energy analysis (SEA), The Winter Annual Meeting of the American Society of Mechanical Engineers, Massachusetts USA, 13–18 December, 1987.
[29] B.R. Mace, Energy flow and s. e.a. at low modal overlap, Fifth International Congress on Sound and Vibration, Adelaide, Australia, December, 1997.
[30] T.D. Scharton, R.H. Lyon, Power flow and energy sharing in random vibration, The Journal of the Acoustical Society of America 43 (1968) 1332–1343.
[31] L. Maxit, J.-L. Guyader, Structural vibration analysis of the CLIO II firewall using SEA model and CLF-DMF technique, NOVEM Meeting, Lyon, France, September, 2000.
[32] J.-L. Guyader, State of the art of energy methods used for vibro acoustic predictions, Sixth International Congress on Sound and Vibration, Copenhagen, Denmark, 5–8 July, 1999.
[33] W. Soedel, Vibrations of Shells and Plates, 2nd edition, Marcel Dekker, New York, 1993.